DOE/PC/93225-7

TECHNICAL PROGRESS REPORT

FOR

"HIGH PERFORMANCE MATERIALS IN COAL CONVERSION UTILIZATION"

For The Period
April 1, 1995 - June 30, 1995

July 1995

Work Performed Under Contract No. DE-FG22-93PC93225

Prepared for:
The United States Department of Energy

Prepared by:
The University of Tennessee Space Institute
B. H. Goethert Parkway
Tullahoma, Tennessee 37388-8897

RECEIVED
USDOE/PETC
95 AUG -2 AM 11:25
ACQUISITION & ASSISTANCE DIV.

US/DOE Patent Clearance is Not required prior to publication of this document.

MASTER

DISTRIBUTION OF THIS DOCUMENT IS UNLIMITED

Table of Contents

DISCLAIMER

This report was prepared as an account of work sponsored by an agency of the United States Government. Neither the United States Government nor any agency thereof, nor any of their employees, makes any warranty, express or implied, or assumes any legal liability or responsibility for the accuracy, completeness, or usefulness of any information, apparatus, product, or process disclosed, or represents that its use would not infringe privately owned rights. Reference herein to any specific commercial product, process, or service by trade name, trademark, manufacturer, or otherwise does not necessarily constitute or imply its endorsement, recommendation, or favoring by the United States Government or any agency thereof. The views and opinions of authors expressed herein do not necessarily state or reflect those of the United States Government or any agency thereof.

List of Figures

List of Tables

1.0 INTRODUCTION

This is the seventh quarterly report on a three year grant regarding "High Performance Materials in Coal Conversion Utilization." The grant is for a joint university/industry effort under the US Department of Energy (DOE) University Coal Research Program. The University of Tennessee Space Institute (UTSI) is the prime contractor and The University of Pennsylvania and Lanxide Corporation are subcontractors.

UTSI has completed the planned laboratory exposure tests involving pulverized coal slag on the production of Lanxide DIMOX™ ceramic composite material. In addition, the strength testing (at temperature) of C-ring sections of the production composite is complete and the analysis of the data is reported in a thesis which was submitted toward a M.S. degree.

2.0 DISCUSSION

2.1 Objective and Scope of Work

The object of this grant is to test, analyze, and improve the heat and coal-slag corrosion resistance of a $SiC_{(p)}/Al_2O_3$ ceramic composite tubular material. The material will be evaluated for its ability to withstand the pressures, temperatures and corrosion attack which would be encountered within a coal-fired high-temperature, high pressure air heater. The evaluation will include strength testing at elevated temperatures. The feasibility of several joining and coating techniques will also be investigated.

2.2 Task 1 - Materials (Lanxide Corporation)

Under Lanxide's cost share portion of the grant, they have provided 21 183 cm (six foot), 5 cm (two inch) OD $SiC_{(p)}/Al_2O_3$ DIMOX™ ceramic composite tubes for testing by UTSI. The first 15 tubes were produced in a horizontal furnace and the final six tubes were produced in a vertical furnace.

Previously, SiC particle reinforced alumina matrix composite tubes were fabricated for this program by the DIMOX™ directed metal oxidation process as follows. In a first processing step, tubular SiC preforms were made via slip casting, i.e., the pouring of a SiC slip into plaster molds. After several minutes of build-up of SiC particles on the plaster walls, the residual slip was decanted, and the SiC preform tubes were removed from the plaster mold. Prefiring of the SiC tubes was performed to increase their strength. Subsequently, the alumina matrix growth was performed, using either an inside-out or outside-in lay-up. The described method of preforming via slip casting has several potential disadvantages, which are: the limited life of the plaster mold, the cycle time, and the need for using small particles in the slip in order to keep the larger particles suspended. These small SiC particles oxidize readily during prefiring and matrix growth, thus effectively reducing the SiC volume loading.

However, a high loading is desired in many cases to assure high thermal conductivity, a low coefficient of thermal expansion (CTE), and high thermal shock resistance of the composite tubes. A final disadvantage of slip casting is the limitation in making uniformly round tubes with very thin walls.

In this reporting period we have started to develop an alternate preforming technique that can potentially overcome the listed limitations of slip casting. The new approach utilizes the principles of centrifugal casting. We are planning to fill a cylindrical mold cavity with a mixture of SiC particles and Lanxide's novel preceramic polymer, CERASET™ SN. During the spinning of the mold the SiC particles are forced radially outward. The spaces between the particles are at this point filled with the preceramic polymer. Upon heating of the spinning mold, the preceramic polymer cures to form a rigid material. Upon cooling of the mold, a hard and strong preform can be taken from the mold. Further heating of the preform will convert the cured preceramic polymer into a ceramic.

The potential advantages of centrifugal preforming are manifold. The need for using very small particles (used in slip casting) no longer exists. The preform fabrication times are potentially shorter and mold lifetime is expected to be considerably longer than for plaster molds. It should be possible to produce uniformly round preforms with very thin walls. The strength of these preforms should be quite high. Obviously, these advantages are potential in nature and need to be demonstrated on this program.

The CERASET™ SN preceramic polymer is considerably more advantageous to use than other known commercial or developmental preceramic polymers in that it is solvent free and thermosetting, and features low viscosity, high purity, and excellent stability in ambient atmospheres. Further, the CERASET™ SN polymer is inexpensive and available in large quantities.

To date, the design of a centrifugal tube casting machine has been completed. Orders for all essential components have been placed and some parts have been delivered. Once all components have arrived, the casting machine will be installed and casting trials will commence.

2.3 Task 2 - Pre and Post Test Material Characterization

2.3.1 Subtask 2A - Strength of Materials Testing and Analysis (UTSI)

2.3.1.1 Experiment Procedure

Physical features such as amount and distribution of porosity have strong influence on the mechanical properties of ceramics. A phase image analysis system that consists of an optical microscope and a computer with the software NIH (National Institute of Health) Image 1.52 for studying phase distribution and phase quantitative analysis was performed on as-received, exposed without slag and exposed with slag samples. Samples were cut from those samples that had been earlier subjected to mechanical testing. Two pieces of samples were cut from each

exposed condition. One sample was located on the top side of the tube facing the slag drops and the other was located on the bottom side during the exposure test. Table 1 provides a summary of conditions of analyzed samples. Each sample was metallurgically prepared by polishing with a series of grit papers. The final polishing was done with a 1 μm diamond paste.

In the image analysis system, there is a video camera connected with the microscope interfaced with the computer so that the microstructure image of the sample can be directly transferred to the computer for displaying on the screen of the computer. The image size on the screen for phase quantitative analysis is 205 mm x 160 mm which represents the real area of 229 μm x 293 μm on the sample. In this study, a 40x objective lens and a 10x eyepiece lens were used. The magnification was approximately 700x. The image analysis was conducted at this high magnification (700x) to reduce or eliminate the poor phase contrast effect due to uneven illumination intensity and the non-flat sample surface. These measurements are done in a two dimensional section and readings for an individual image do not represent volume concentrations of the phases. Therefore, the phase measurements were conducted on eight points from the outside wall of the tube to the inside wall. Such measurements provide average phase volume percent throughout the tube wall thickness. The distance between the points is about 685 μm.

2.3.1.2 Results and Discussion

After obtaining the image of the required location on the computer screen, the program NIH Image 1.52 was used to obtain the individual phase volume percent. Figure 1 illustrates one such typical image used to conduct image analysis. Table 2 gives the measurements of all 13 samples.

From Table 2, it is obvious that the phase distributions of the as-received samples are almost uniform along the cross section of the tube. After the samples were exposed at high temperature, however, the phase distributions were not uniform within the sample, especially for aluminum and porosity content. The more severe the exposure condition, the more porosity and the less dispersed aluminum near the surface of the tube.

Figures 2-5 are plots of the average phase volume data in Table 2. Figures 2 and 3 show the change of aluminum and alumina as a function of exposure temperature. The top side of the sample exposed to slag at 1400°C shows a substantial increase (~ 32%) in aluminum content and a decrease (~ 11%) in alumina compared to that of the as-received sample at room temperature. It is possible that reduction reaction of alumina occurred and part of alumina reduced to aluminum at the 1400°C-with slag case. The general variation trends in SiC and porosity can be seen from Figures 4 and 5. The SiC volume fraction will decrease and the porosity will increase with the increase of temperature and the addition of slag. It may be considered that the reduction of SiC results in the increase of porosity. It is apparent

Table 1. Conditions of analyzed samples.

Sample Number	Exposure Temperature	Exposure condition	Sample Location	Characteristic Strength[1] σ_o
0#	As-received	----------	----------	410 MPa
1#	1100 °C/200 hours	No Slag	Top	282 MPa
2#	1100 °C/200 hours	No Slag	Bottom	282 MPa
3#	1100 °C/200 hours	With Slag	Top	245 MPa
4#	1100 °C/200 hours	With Slag	Bottom	245 MPa
5#	1260 °C/200 hours	No Slag	Top	226 MPa
6#	1260 °C/200 hours	No Slag	Bottom	226 MPa
7#	1260 °C/200 hours	With Slag	Top	328 Mpa
8#	1260 °C/200 hours	With Slag	Bottom	328 MPa
9#	1400 °C/200 hours	No Slag	Top	197 MPa
10#	1400 °C/200 hours	No Slag	Bottom	197 MPa
11#	1400 °C/200 hours	With Slag	Top	149 MPa
12#	1400 °C/200 hours	With Slag	Bottom	149 MPa

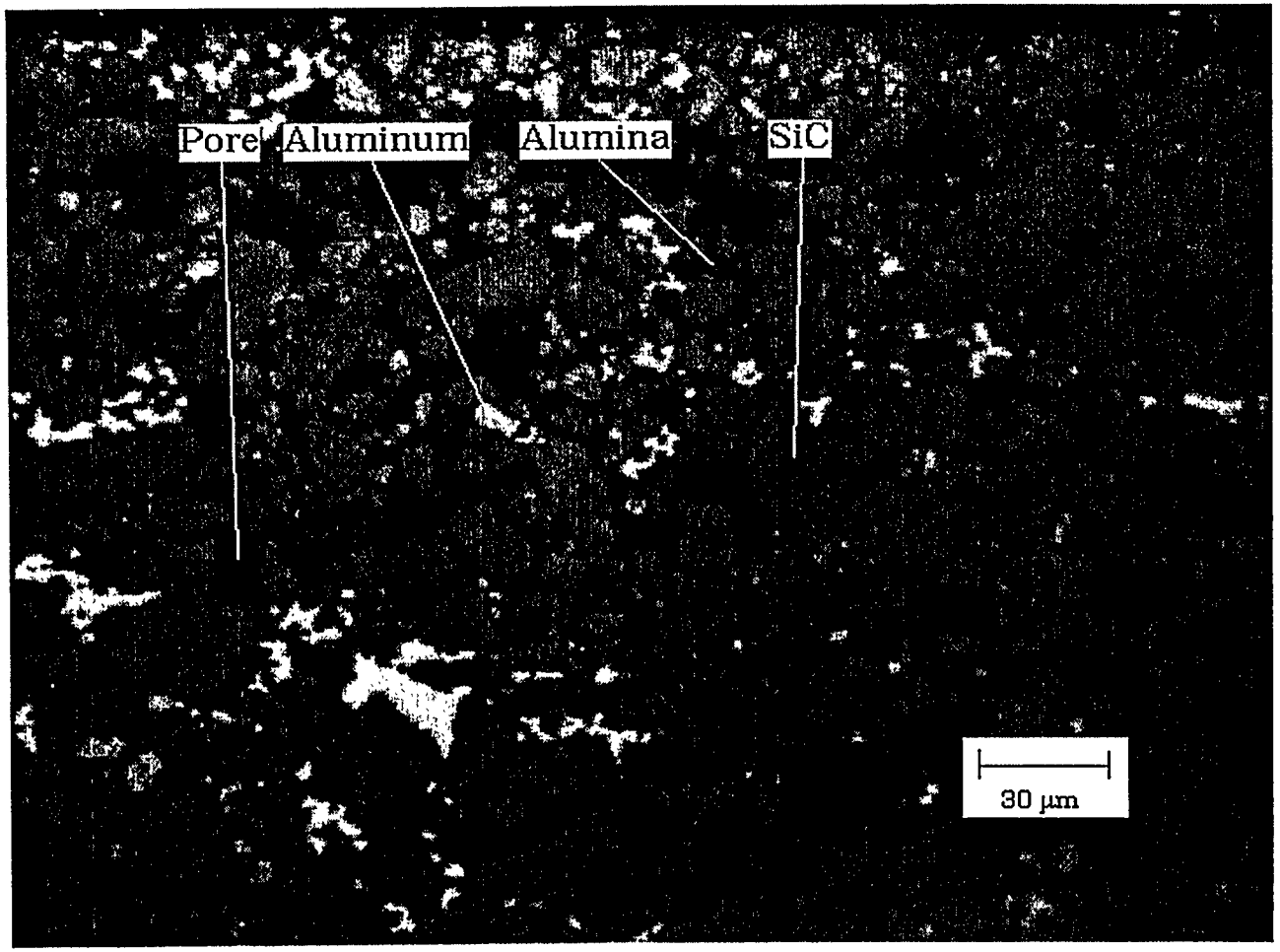

Figure 1. A microstructure image of sample 11# in middle area of cross section.

Table 2. The measurement for phase volume percent (%).

0# -- As received				
	Aluminu	SiC	Alumina	Pore
Out Wall	4.334961	42.98698	50.24251	2.435547
.	3.326823	48.05794	46.85286	1.76237
.	3.232096	49.74805	45.73014	1.289714
.	3.336914	51.73242	43.82324	1.264648
.	3.728841	57.2679	38.0612	0.740234
.	3.574219	53.51986	41.86068	1.045247
.	3.724284	53.87988	40.57227	1.823568
Inside Wal	3.668294	54.26465	42.44271	0.971354
Average:	***3.6158***	***51.4322***	***43.6982***	***1.41659***

1# -- Exposed at 1100 °C without slag (top)				
	Aluminum	SiC	Alumina	Pore
Out Wall	2.968099	51.83496	41.76563	3.431315
.	3.426758	49.96094	44.55273	2.05957
.	3.35319	49.28158	46.22493	1.140299
.	3.272135	50.22493	44.80013	1.702799
.	2.653646	49.44987	45.15951	2.736979
..	4.568359	51.75977	43.23828	0.433594
.	4.464844	51.97624	41.27995	2.558919
Inside Wall	3.950521	50.7819	42.39225	2.875326
Average:	***3.58219***	***50.6588***	***43.6767***	***2.11735***

2# -- Exposed at 1100 °C without slag (bottom)				
	Aluminum	SiC	Alumina	Pore
Out Wall	1.707357	46.18424	47.63379	4.474609
.	2.784505	45.84603	49.0599	2.30957
.	2.417643	48.97298	46.43848	2.170898
.	2.55599	49.53125	45.42806	2.484701
.	3.406576	49.68555	45.2028	1.705078
.	3.617188	51.19792	43.45475	1.730143
.	5.964844	50.8431	42.02702	1.165039
Inside Wall	3.030599	47.91016	45.08268	3.976563
Average:	***3.18559***	***48.7714***	***45.5409***	***2.50208***

3# -- Exposed at 1100 °C with slag (top)				
	Aluminum	SiC	Alumina	Pore
Out Wall	2.226563	47.09668	48.4554	2.221354
.	2.979167	51.17383	44.47949	1.367513
.	2.8125	51.57031	44.28483	1.332357
.	3.148438	49.22168	43.06771	4.562174
.	3.084635	50.43066	43.84342	2.641276
.	3.459961	52.72233	41.95475	1.862956
.	2.927734	50.39421	42.36751	4.310547
Inside Wall	2.838867	52.57324	42.46387	2.124023
Average:	***2.93473***	***50.6479***	***43.8646***	***2.55278***

4# -- Exposed at 1100 °C with slag (bottom)				
	Aluminum	SiC	Alumina	Pore
Out Wall	2.708659	46.7347	46.5013	4.055339
.	3.193034	47.41439	46.32552	3.067057
.	2.456706	51.38965	43.85059	2.30306
.	3.422201	51.14616	43.91081	1.520833
.	4.650065	50.62858	43.64421	0.77181
.	4.097331	49.56152	44.32194	2.361003
.	3.597005	51.95378	42.21908	2.230143
Inside Wall	2.587565	47.69434	44.86784	5.366536
Average:	***3.33907***	***49.5654***	***44.4552***	***2.70947***

Table 2. continues

5# -- Exposed at 1260 °C without slag (top)				
	Aluminum	SiC	Alumina	Pore
Out Wall	1.433268	45.94466	44.45117	8.170898
.	1.101563	42.61393	47.71582	8.568685
.	3.238281	45.72591	45.8431	5.192708
.	3.383789	47.24186	43.92188	5.452474
.	4.472656	50.80176	42.92448	1.801107
.	3.719076	51.50521	42.75	2.025716
.	3.202148	43.87272	45.18945	7.735677
Inside Wall	3.378255	46.18555	43.20475	7.848307
average:	***2.99113***	***46.7365***	***44.5001***	***5.84945***

6# -- Exposed at 1260 °C without slag (bottom)				
	Aluminum	SiC	Alumina	Pore
Out Wall	1.603841	45.68327	46.90234	5.810547
.	2.359049	47.58431	45.95475	4.101888
.	4.3125	48.96582	42.65592	4.065755
.	3.762695	51.61133	40.86719	3.145508
.	4.547526	49.86686	41.14876	4.436849
.	4.668945	49.1097	42.63281	3.09375
.	2.683251	49.16081	42.33464	5.821299
Inside Wall	2.798828	49.65853	44.18945	3.35319
Average:	***3.34208***	***48.9551***	***43.3357***	***4.2286***

7# -- Exposed at 1260 °C with slag (top)				
	Aluminum	SiC	Alumina	Pore
Out Wall	2.091797	43.54785	48.25944	6.100911
.	2.738932	48.89453	46.92676	1.439779
.	4.203776	48.53288	45.12077	2.142578
.	2.50944	47.4401	46.52018	3.530273
.	4.372396	49.24837	44.34831	2.030924
.	2.735352	46.8265	48.34147	2.09668
.	2.486328	46.15788	48.42611	1.701497
Inside Wall	2.857747	46.68815	47.5179	2.936198
average:	***2.99947***	***47.167***	***46.9326***	***2.74736***

8# -- Exposed at 1260 °C with s+G20lag (bottom)				
	Aluminum	SiC	Alumina	Pore
Out Wall	1.461914	45.73926	45.54818	7.250651
.	3.873372	46.98763	45.55664	3.582357
.	3.113281	49.96029	44.26758	2.658854
.	3.768556	47.97363	45.37728	2.880534
.	2.347656	49.51888	46.19857	1.934896
.	2.353841	47.89811	47.5918	2.15625
.	3.098633	49.46094	44.13216	3.308268
Inside Wall	3.418294	45.16374	47.99219	3.425781
average:	***2.92944***	***47.8378***	***45.8331***	***3.3997***

9# -- Exposed at 1400 °C without slag (top)				
	Aluminum	SiC	Alumina	Pore
Out Wall	1.802083	45.00749	42.68327	5.366211
.	2.268229	46.71354	44.34635	6.671875
.	4.169922	49.09147	39.34115	7.397461
.	5.451823	48.37663	41.15951	5.012044
.	6.155924	48.81706	39.93294	5.094076
.	3.405924	49.23079	44.3112	3.052083
.	4.173177	49.8763	41.82422	4.126302
Inside Wall	2.773763	46.33301	44.21159	6.681641
average:	***3.77511***	***47.9308***	***42.2263***	***5.42521***

10# -- Exposed at 1400 °C without slag (bottom)				
	Aluminum	SiC	Alumina	Pore
Out Wall	3.996094	46.80762	41.0446	8.151693
.	5.734375	49.45247	41.02116	3.791992
.	1.742513	48.27116	44.85319	5.133138
.	3.272461	47.75586	44.50716	4.464518
.	4.361979	48.86784	39.79492	6.97526
.	3.02832	51.0638	41.73535	4.172526
.	2.719727	50.00033	43.06673	4.294271
Inside Wall	2.757813	48.58659	42.9668	5.688802
average:	***3.45166***	***48.8507***	***42.3737***	***5.33403***

11# -- Exposed at 1400 °C with slag (top)				
	Aluminum	SiC	Alumina	Pore
Out Wall	3.688151	47.81217	40.8151	7.684579
.	3.829102	47.41927	39.70833	7.876302
.	5.046224	46.31934	40.89941	7.735026
.	3.669915	47.50814	39.29688	9.525065
.	5.51888	48.97396	36.19824	9.308919
.	5.554036	47.36621	39.6556	7.424154
.	7.385417	48.7679	36.4821	7.364583
Inside Wall	3.652018	46.67025	39.51563	10.16211
average:	***4.79297***	***47.6047***	***39.0714***	***8.38509***

12# -- Exposed at 1400 °C with slag (bottom)				
	Aluminum	SiC	Alumina	Pore
Out Wall	1.887044	43.63509	42.30859	12.16927
.	2.329427	43.54525	45.40462	8.720703
.	3.498047	44.50488	43.01986	8.977214
.	2.286133	43.02767	44.25586	9.231445
.	3.401367	42.98145	45.47461	8.142578
.	2.061523	45.67122	43.78906	8.47819
.	4.575846	46.49121	42.48405	5.863932
Inside Wall	3.603516	45.91895	41.05892	9.41862
average:	***2.95536***	***44.472***	***43.4745***	***8.87524***

Average Volume Percent Value of Aluminum (%)					
	As-received	Top-no slag	Bottom-no slag	Top-slag	Bottom-slag
Room Temperature	3.6158				
1100 oC		3.58219	3.18559	2.93473	3.33907
1260 oC		2.9913	3.34208	2.99947	2.92944
1400 oC		3.77511	3.45166	4.79297	2.95536

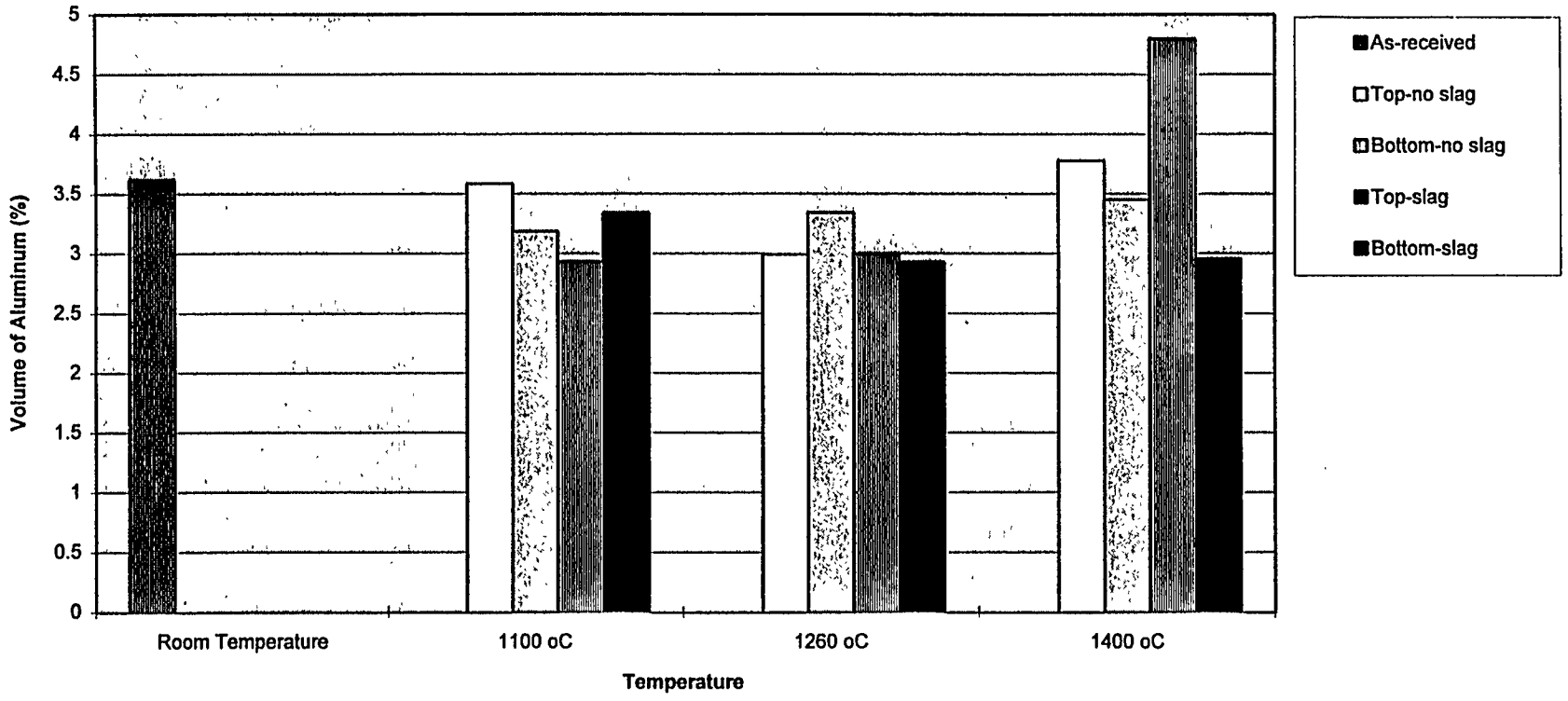

Figure 2. Aluminum content vs. exposure conditions

	Average Volume Percent Value of Alumina (%)				
	As-received	Top-no slag	Bottom-no slag	Top-slag	Bottom-slag
Room Temperature	43.6982				
1100 oC		43.6767	45.5409	43.8646	44.4552
1260 oC		44.5001	43.3357	46.9326	45.8331
1400 oC		42.2263	42.3737	39.0714	43.4745

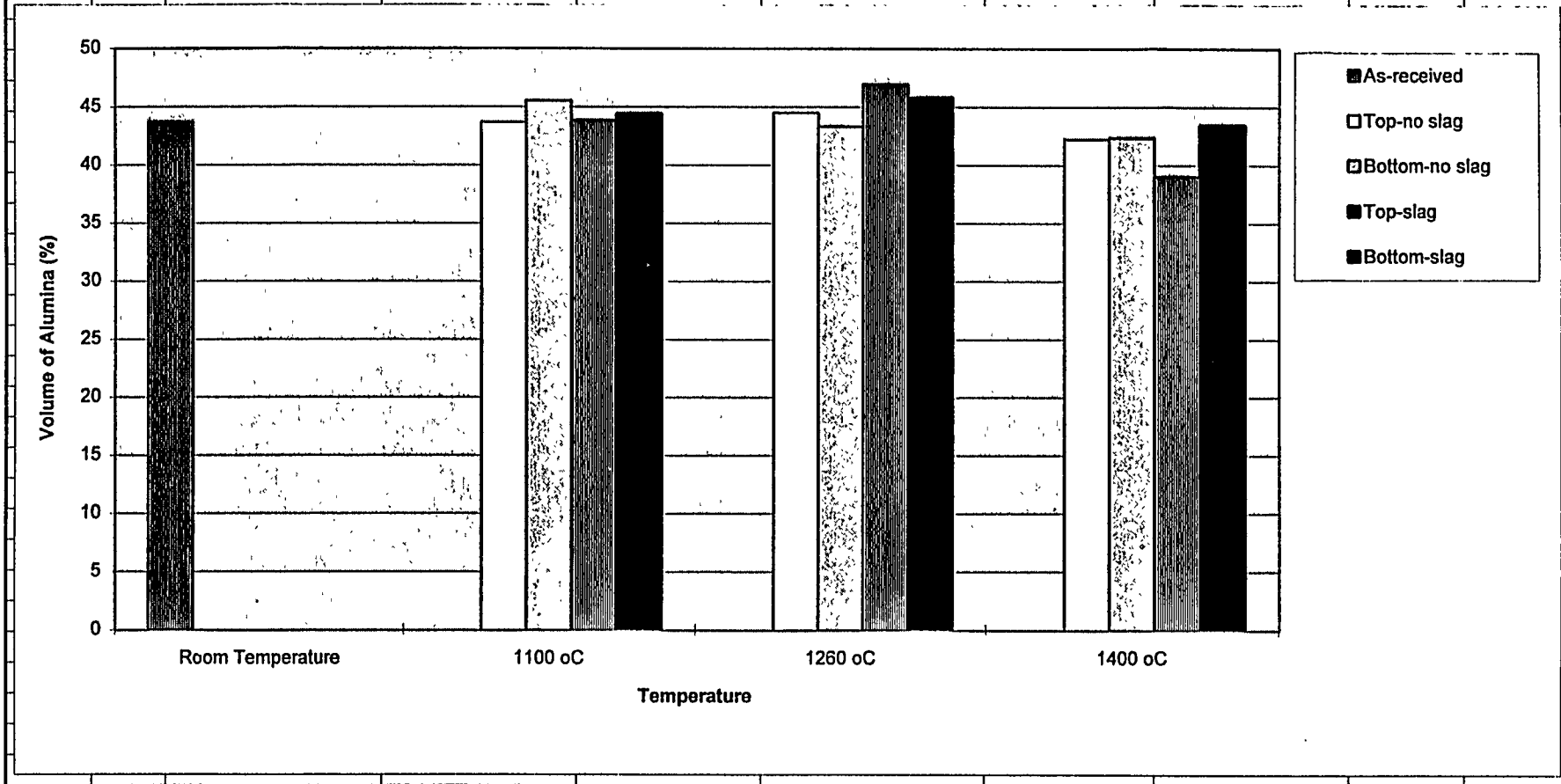

Figure 3. Alumina content vs. exposure conditions

	Average Volume Percent Value of SiC (%)				
	As-received	Top-no slag	Bottom-no slag	Top-slag	Bottom-slag
Room Temperature	51.4322				
1100 oC		50.6588	48.7714	50.6479	49.5654
1260 oC		46.7365	48.9551	47.167	47.8378
1400 oC		47.9308	48.8507	47.6047	44.472

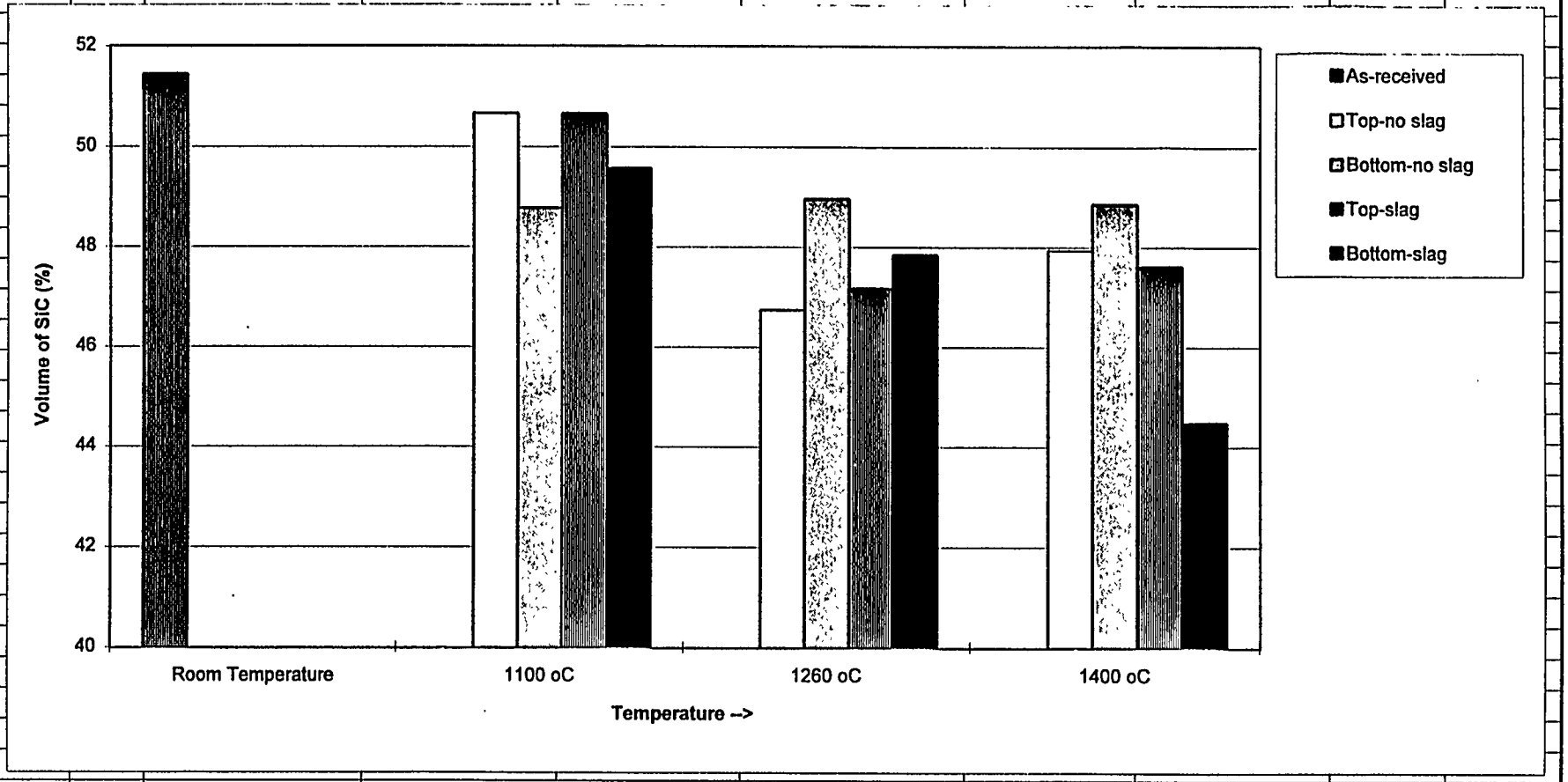

Figure 4. SiC content vs. exposure conditions

Average Volume Percent Value of Pore (%)					
	As-received	Top-no slag	Bottom-no slag	Top-slag	Bottom-slag
Room Temperature	1.41659				
1100 oC		2.11735	2.50208	2.55278	2.70947
1260 oC		5.84945	4.2286	2.74736	3.3997
1400 oC		5.42521	5.33403	8.38509	8.87524

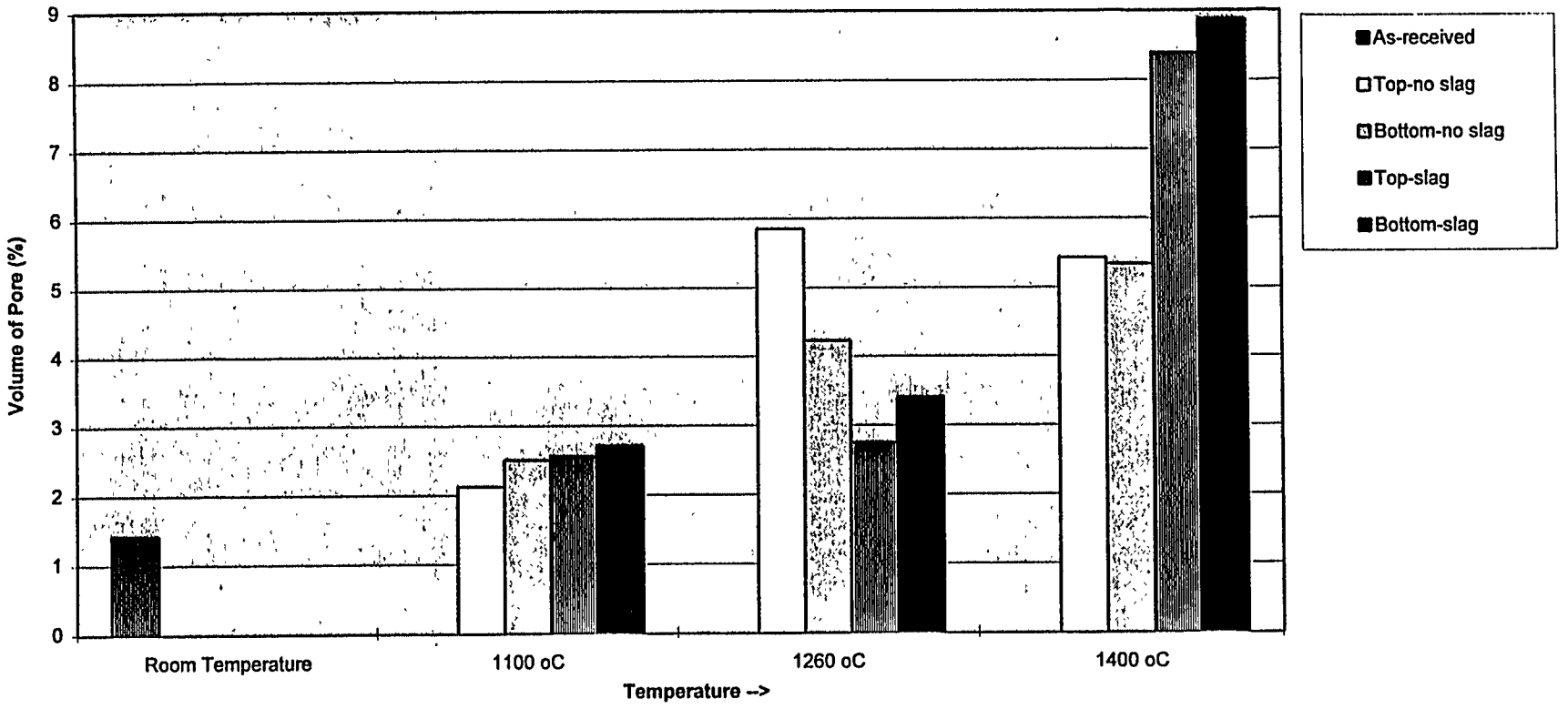

Figure 5. Porosity content vs exposure conditions

that the increase of porosity will lead to the decrease of the strength. Figure 6 shows the variation trend in the strength with exposure conditions. As expected, an increase in exposure temperature results in more loss of strength and material. Also, the material not exposed to slag is stronger than material exposed to slag at the same temperature. But the porosity variation trend with the exposure condition is just the reverse of the strength variation. However, there is an exception for the material exposed to slag at 1260°C, showing an anomalous behavior. It appears stronger than it should be based on its exposure condition.

The explanation for this unexpected result is related to the nature of the slag coating on the material test C-rings that were produced at 1260°C. Those tubes which were exposed to slag at this temperature developed a thick, hard, glassy, bubble filled slag layer which was firmly bonded to the tube surface. Before cutting the mechanical test specimens, most of this slag was removed. However, it was not possible to remove all of the slag without damaging the base material. Therefore, after cutting and grinding the test specimens, there was a slag layer approximately I mm thick on the specimens. This remaining slag layer provided a significant amount of additional strength to the test sample during mechanical testing[2].

There was also an anomalous behavior for porosity content of material exposed at 1260°C with slag. It showed less porosity than expected considering the exposure condition. Figure 7 contains micrographs of surface appearances of the specimens after exposure to high temperatures with slag. Slag on the tube exposed to 1100°C is still friable and it is easy to remove. Figure 7-(a), shows that there was a layer of alumina coating, produced by the manufacturer, filling pores and no slag remains on the surface. Figure 7-(b) shows a layer of pore free slag firmly bonded onto the layer of alumina coating. The slag also infiltrated into the alumina coating and hence sealed the pores on the alumina layer. This is equivalent to sealing up the micro-cracks on the surface of the tube. In addition, this made it more difficult for oxygen to diffuse into the substrate material so that fewer pores were produced. All of these factors would contribute to the increase of strength.

Figure 7 (a) and (b) indicate little or no material loss and no reaction with slag at 1100°C and 1260°C with slag. Only noticeable loss of material occurred at 1400°C with slag. Figure 7-(c) shows that the alumina coating has totally disappeared. (Apparently a reaction product remained on the substrate material.) After exposure to slag at 1400°C, the thickness of the tube on the top side was 3.24 mm and the bottom side was 4.6 mm. The average thickness of the as received tube was about 4.7 mm. This indicates that more material loss occurred on the top side which received slag directly than that on the bottom side. Examination of the sample exposed at 1400°C without slag, showed a small amount of material loss. This suggests that there must be some reaction between the substrate material and slag at 1400°C to form a low melting eutectic. The slag used in this study contained more than 10 percent of CaO (in other similar experiments, the CaO content in the slag that

	Characteristic Strength (MPa)		
	As-received	no slag	with slag
Room Temperatur	410		
1100 oC		282	245
1260 oC		226	328
1400 oC		197	149

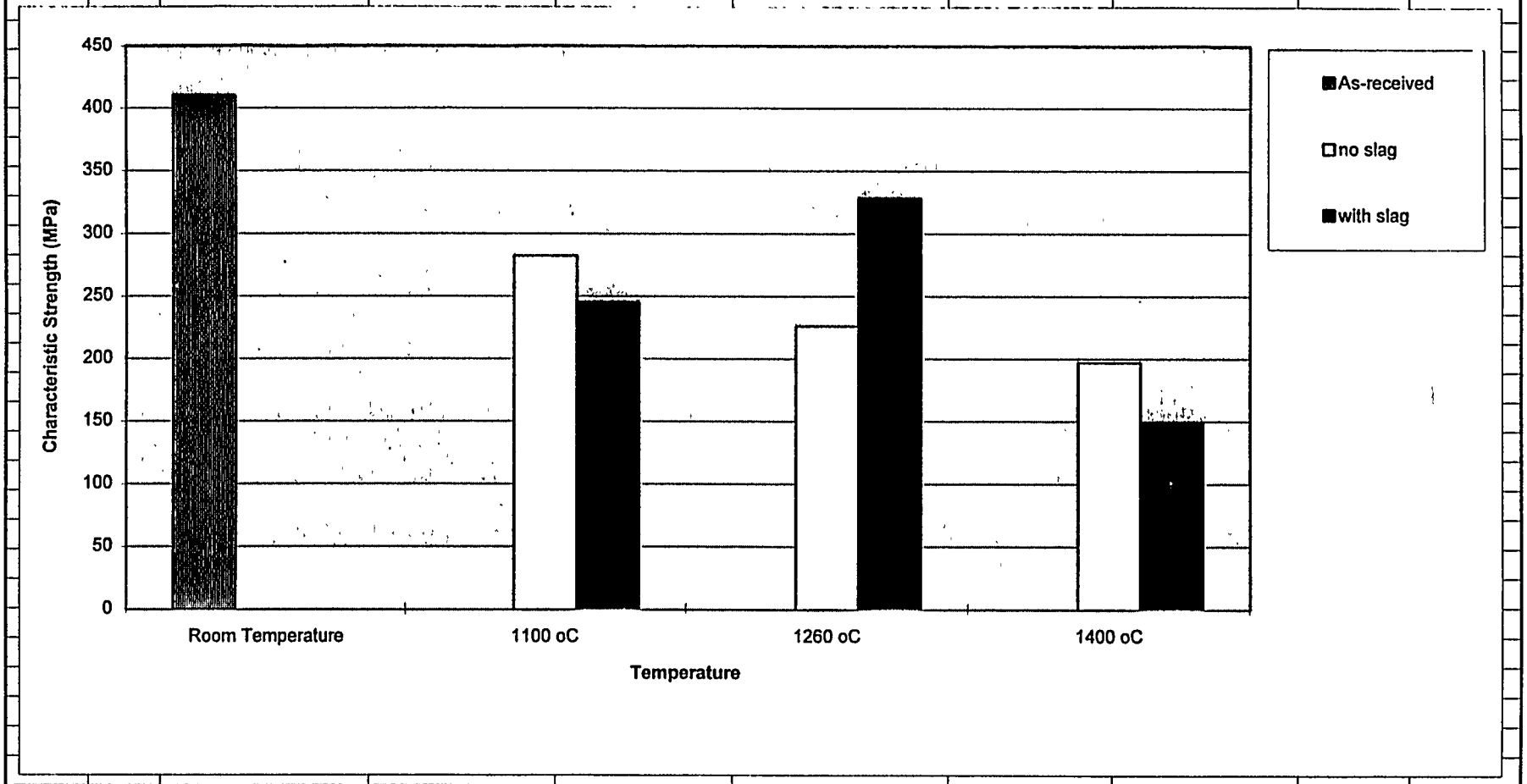

Figure 6. Characteristic strength vs. exposure conditions

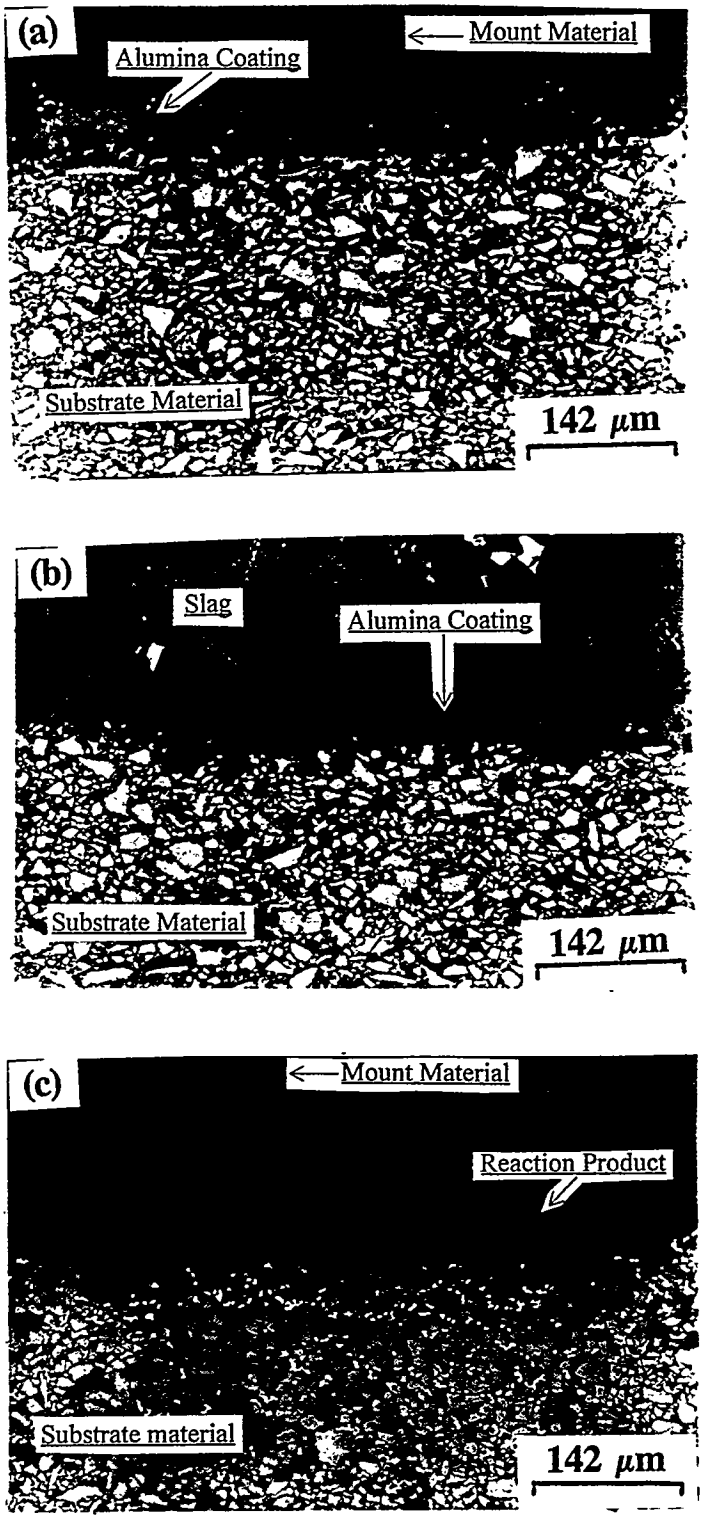

Figure 7. Cross section views of samples exposed to slag at high temperature. (a) sample 3# / 1100 °C with slag; (b) sample 7# / 1260 °C with slag; (c) sample 11# / 1400 °C with slag;

came from the MHD furnace was more than 20%[3]). Table 3 gives the slag composition[4]. According to the phase diagram illustrated in Figure 8, Al_2O_3 will react with CaO (at ~50 wt.%) to form a low melting eutectic which melts at or above 1360°C. In addition, silicon has a stronger affinity towards oxygen, therefore it forms a thin layer of silicon dioxide (SiO_2) on the surface of the silicon carbide. When exposed to high temperatures, such a SiO_2 layer could react with Al_2O_3 and CaO forming a lower melting eutectic (1265°C) according to the phase diagram in Figure 9. It is felt that the main reason for material loss at 1400°C-with slag is due to the formation of the low melting eutectic. It is predicted that if this material is used below 1265°C with the slag used in this study, there should be no noticeable material loss occurring.

Table 3. Test slag composition (%)

Compound	Relative Amount (by mass)
SiO_2	47.76
Fe_2O_3	19.79
Al_2O_3	16.57
CaO	10.37
MgO	2.62
K_2O	1.48
TiO_2	0.85
Na_2O	0.37
SO_3	0.19

2.3.2 Subtask 2B - Corrosion Thermodynamic Analysis (U of Pa)

Attempts at developing a fundamental kinetic model for the corrosion of the DIMOX™ material have had limited success. As shown in Figure 10, the viscosity (and hence diffusivity) of silicate solutions changes significantly with cation contamination. This behavior is shown in the present study by the stark changes in slag viscosity over the temperature ranges used. This sensitivity requires actual diffusion data for the target slag materials. Additionally, since the oxidation process and reaction at the slag/composite interface will change the local composition of the scale, a time and depth dependent diffusivity must be used. The lack of available diffusion data have made the development of a predictive model impossible at present. Finally, there is a lack of reaction rate data for the residual metal phase. Since this phase is expected to corrode rapidly, leading to strength degrading flaws, the focus has been toward modeling the corrosion of the residual Al-Si alloy. Pertinent corrosion data for

$CaO–Al_2O_3$

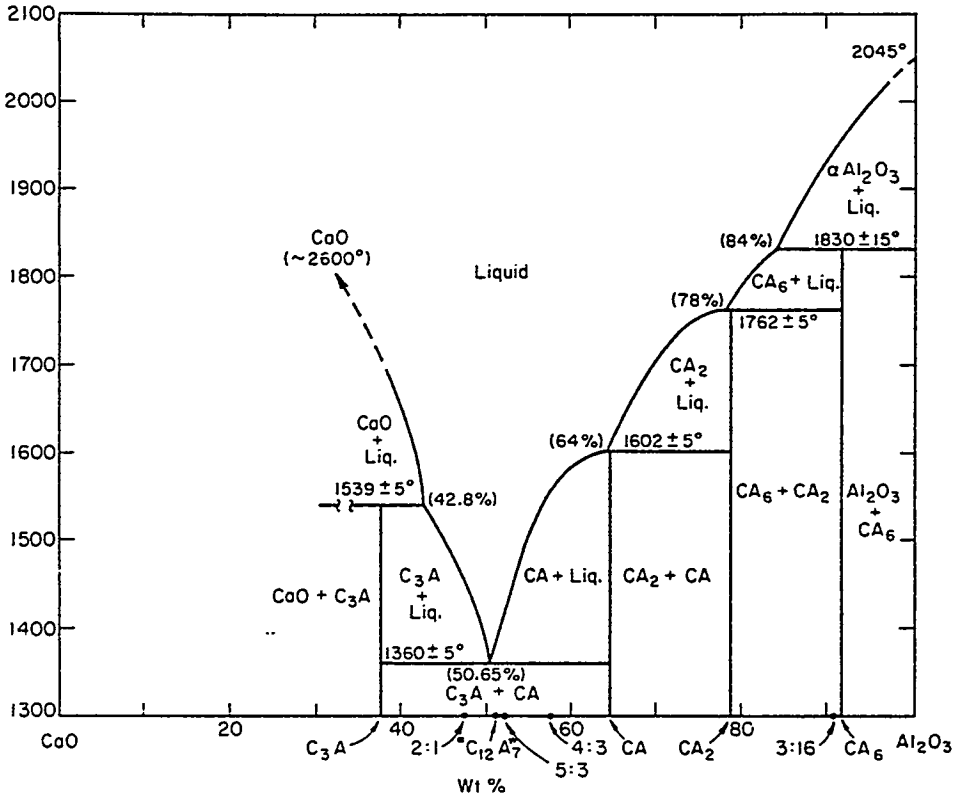

Figure 8. The phase diagram of system CaO - Al_2O_3 [5]. A = Al_2O_3, C = CaO.

$CaO–Al_2O_3–SiO_2$

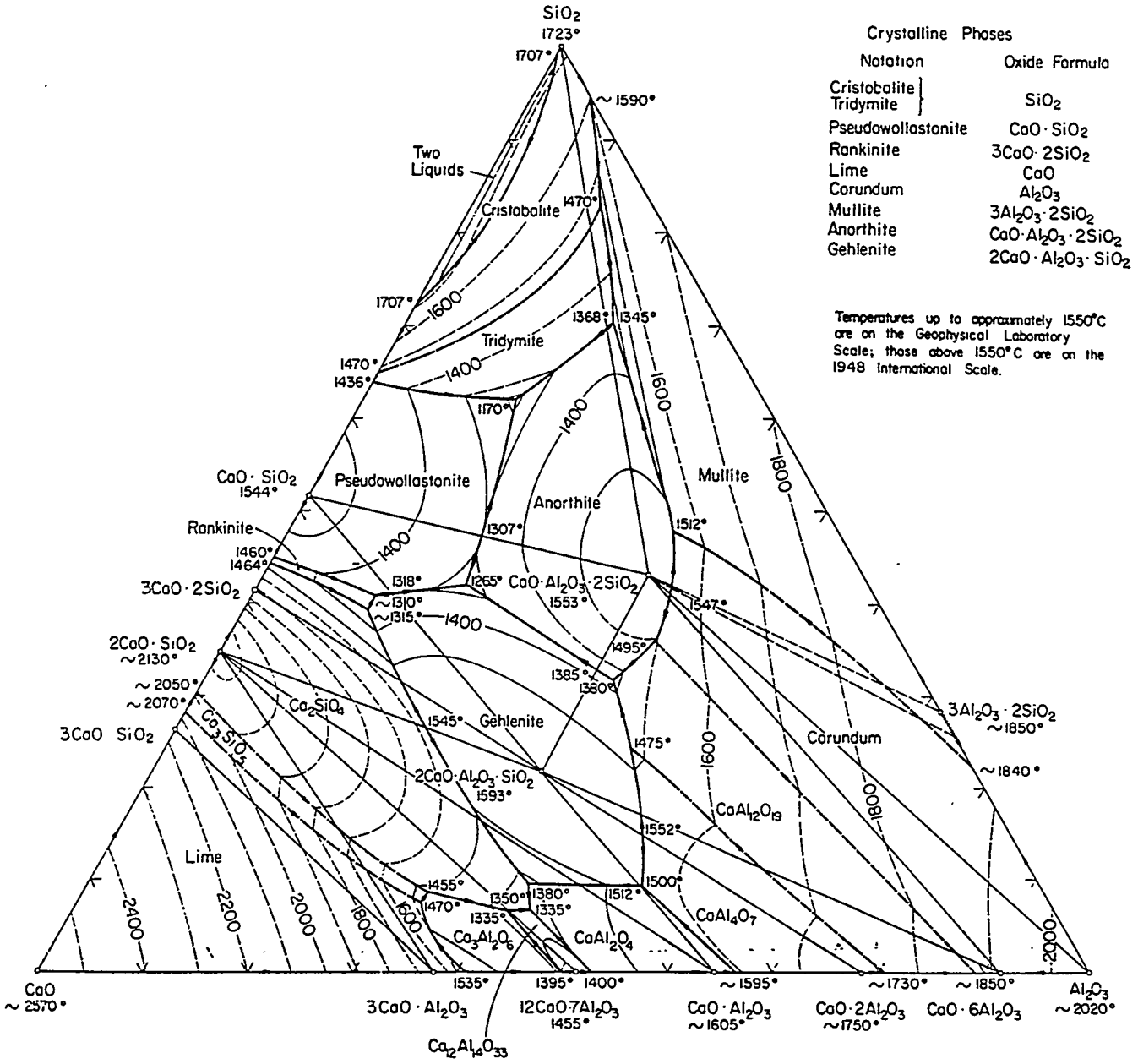

Figure 9. The phase diagram of system $CaO - Al_2O_3 - SiO_2$ [6].

incorporation into the model has not been found. At this point, it appears that the system is too complex to model without more assessed kinetic data. The results of the UTSI analysis will be incorporated into the computer model which will, hopefully, fill the voids in the data and yield valid corrosion predictions.

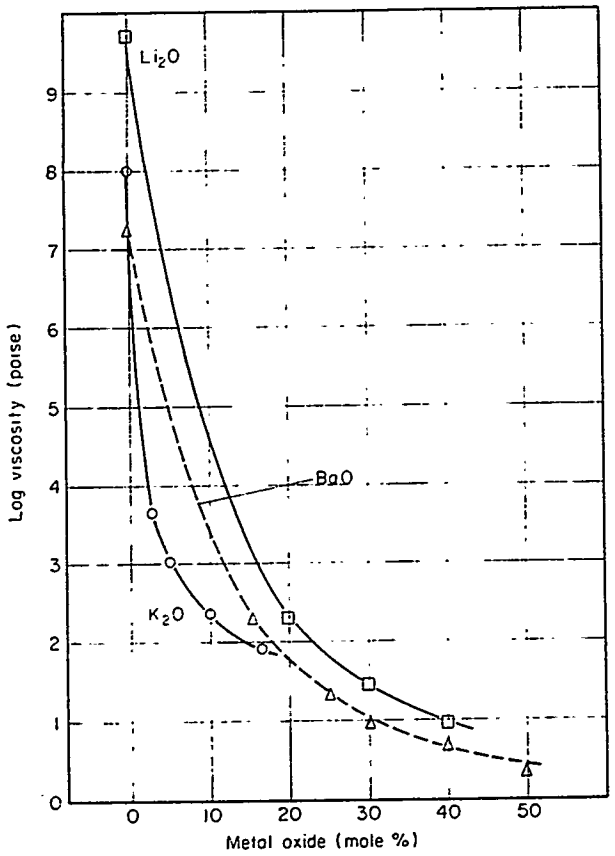

Figure 10. The viscosities of 3 binary silicates shown as a function of composition; $Li_2O + SiO_2$ at 1400°C, $K_2O + SiO_2$ at 1600°C, and $BaO + SiO_2$ at 1700°C. From Physical Chemistry of Melts in Metallurgy, Volume 1, F.D. Richardson, Academic Press p. 93 (1974)

2.4 Task 3 - Exposure Testing

2.4.1 Subtask 3A - Bench Scale Lab Tests (UTSI)

The remaining bench scale expose tests will involve the tube produced by Lanxide involving the preceramic polymer described in Paragraph 2.2. This tube will be exposed to coal slag for 200 hours at 1260°C. At the conclusion of the test the tube will be cut into 20 C-ring sections, strength tested at 1260°C and the results compared to results from the similarly exposed DIMOX™ tube.

2.4.2 Subtask 3B - Field Exposure Tests (UTSI)

The termination of the MHD program has limited field testing to the five tubes previously exposed during the final MHD test. Since these tubes seem to be of less interest due to the potassium seed added to the coal flow, UTSI is devoting most of their effort to the bench scale tests. Dr. Ken Natesan of the Energy Technology Division at Argonne National Laboratory has offered to perform a corrosion analysis on the field-tested tubes. (It was pointed out at the recent Materials Conference in Oak Ridge, that NO_X emission controls would likely lead to High Temperature Heat Exchangers that must operate in a reducing environment. Most of the field tested tubes were in a reducing environment so that an analysis of these tubes may still be of value.) The results of Dr Natesan's analysis will be included in a future quarterly report.

2.5 Task 4 - Project Management

Mr. Bill Boss attended the Materials Conference In Oak Ridge, TN. Mr. Boss also presented a review of this grant at the University Coal Research Contractor's Review Conference in Nashville, TN. on June 14, 1995.

Mr. Peter LaRue successfully defended his thesis and graduated with a M.S. Degree in Mechanical Engineering in May 1995.

UTSI was notified that the DOE Conract Monitor, Mr.Cliff Smith, was replaced by Mr. Andy Karesh.

3.0 SCHEDULE

The project is on schedule in that all the lab tests on the production composite material have been completed by UTSI. Lanxide is on schedule regarding the manufacture of their prototype of their new product. The U of Pa is having difficulty is in modelling the corrosion mechanism relating to the UTSI tests due to complex chemistry involved.

4.0 CONCLUSION

The overall research continues to go smoothly and most of the objectives are being met at this time within budget. The laboratory high temperature exposure tests by UTSI on the production of Lanxide tube samples are now complete and the strength tests of the exposed samples is also complete. A detailed microstructural analysis of the remains of these tests is currently underway.

Lanxide Corporation is currently fabricating a new 25 cm ceramic composite tube based on their innovative manufacturing process. This tube will be tested by UTSI and compared to the results obtained from their production tubes.

The University of Pennsylvania has experienced difficulty in modelling the corrosion encountered in this program due to the extremely complex conditions present. Test results from UTSI hopefully will enable the University to complete this task.

5.0 REFERENCES

1. P. F. LaRue, MS Thesis, University of Tennessee Space Institute (1996) P. 39.

2. P. F. LaRue, MS Thesis, University of Tennessee Space Institute (1996) P. 43.

3. J. P. Winkler, MS Thesis, University of Tennessee Space Institute (1992) P. 53.

4. P. F. LaRue, MS Thesis, University of Tennessee Space Institute (1996) P. 10.

5. Margie K. Reser, Phase Diagram for Ceramists, P. 103, the American Ceramic Society, 1975 Supplement.

6. Margie K. Reser, Phase Diagram for Ceramists, volume 1, P. 209, the American Ceramic Society. Fifth printing 1985.